Three-dimensional nonlinear evolution of equatorial ionospheric spread-F bubbles

M. J. Keskinen
Charged Particle Physics Branch, Plasma Physics Division, Naval Research Laboratory, Washington, DC, USA

S. L. Ossakow
Plasma Physics Division, Naval Research Laboratory, Washington, DC, USA

B. G. Fejer
Center for Atmospheric and Space Studies, Utah State University, Logan, Utah, USA

Received 27 March 2003; revised 9 May 2003; accepted 10 June 2003; published 26 August 2003.

[1] Using numerical simulation techniques, we present the first study of the three-dimensional nonlinear evolution of an equatorial spread-F bubble. The background ionosphere used to initialize the bubble evolution is computed using a time-dependent first-principles equatorial plasma fountain model together with a prereversal enhancement vertical drift model. We find that finite parallel conductivity effects slow down both the linear and nonlinear bubble evolution compared to the two-dimensional evolution. In addition we find that bubble-like structures with extremely sharp density gradients can be generated off the equator at equatorial anomaly latitudes in agreement with recent observations. *INDEX TERMS:* 2415 Ionosphere: Equatorial ionosphere; 2439 Ionosphere: Ionospheric irregularities; 2447 Ionosphere: Modeling and forecasting; 2471 Ionosphere: Plasma waves and instabilities. **Citation:** Keskinen, M. J., S. L. Ossakow, and B. G. Fejer, Three-dimensional nonlinear evolution of equatorial ionospheric spread-F bubbles, *Geophys. Res. Lett.*, *30*(16), 1855, doi:10.1029/2003GL017418, 2003.

1. Introduction

[2] Equatorial spread-F bubbles,plumes, and depletions are a major class of ionospheric dynamics and structure and are a distinct manifestation of ionospheric weather. Recently, several observational studies both in quiet [*Kelley et al.*, 2002; *Otsuka et al.*, 2002; *Stephan et al.*, 2002; *Chen et al.*, 2001; *Huang et al.*, 2001; *Sahai et al.*, 2000; *Sinha et al.*, 1999; *Kil and Heelis*, 1998; *Basu et al.*, 1996; *Weber et al.*, 1996] and stormtime conditions [*Basu et al.*, 2001a; *Basu et al.*, 2001b; *Yeh et al.*, 2001] of equatorial spread-F have demonstrated the need for a full three-dimensional nonlinear model of the evolution of spread-F bubbles. *Kelley et al.* [2002] have presented ground-based observations of a major equatorial spread-F event from Hawaii which is far from the geomagnetic equator. Their observations showed that bubbles reached altitudes of over 1500 km with strong effects recorded at the Hawaii observing site. *Otsuka et al.* [2002] reported equatorial F-region airglow depletions extending to much higher latitudes off the geomagnetic equator. In stormtime periods, [*Basu et al.*, 2001a; *Basu et al.*, 2001b] demonstrated that strong ionospheric density structures can be observed at equatorial anomaly latitudes during equatorial spread-F events. An outstanding problem is the three-dimensional nonlinear evolution of equatorial spread-F bubbles.

[3] Much work has been performed relating to the two-dimensional nonlinear evolution of equatorial spread-F bubbles and plumes in the equatorial plane [*Scannapieco and Ossakow*, 1976; *Keskinen et al.*, 1980; *Huang et al.*, 1993; *Hysell et al.*, 1994; *Sekar et al.*, 1995]. The quasi-three-dimensional nonlinear evolution of equatorial spread-F bubbles using magnetic flux tube integration techniques [*Zalesak et al.*, 1982; *Keskinen et al.*, 1998] has been studied. Some work on the linear theory of the three-dimensional evolution of equatorial spread-F bubbles [*Basu*, 2002] has been published. However, the full three-dimensional nonlinear evolution of equatorial spread-F bubbles has not been quantified. A fully three-dimensional nonlinear treatment is needed in order to develop quantitative predictive mechanisms for equatorial spread-F and to compare with experimental observations. In this paper we study the three-dimensional nonlinear evolution of equatorial spread-F bubbles using numerical simulation techniques. In section 2 we outline the basic nonlinear bubble model. In addition we describe the background ionospheric model used in the equatorial nonlinear bubble model. In section 3 we give results from the nonlinear bubble simulations. Finally, we summarize and discuss the results.

2. Model

[4] To compute the three-dimensional nonlinear evolution of equatorial spread-F bubbles we use the Mesoscale Ionospheric Dynamics and Assimilation Model (MIDAS) [*Keskinen et al.*, 1998]. MIDAS contains the equations for density, momentum, and current continuity

$$\frac{\partial n_\alpha}{\partial t} + \nabla \cdot n_\alpha \mathbf{V}_\alpha = -\nu_R n_\alpha \tag{1}$$

$$\left(\frac{\partial}{\partial t} + \mathbf{V}_i \cdot \nabla\right)\mathbf{V}_i = \frac{e}{m_i}\left(\mathbf{E} + c^{-1}\mathbf{V}_i \times \mathbf{B}\right) - \nu_{ie}(\mathbf{V}_i - \mathbf{V}_e) - \nu_{in} \cdot (\mathbf{V}_i - \mathbf{U}) + \mathbf{g} \tag{2}$$

$$-\frac{e}{m_e}\left(\mathbf{E} + \frac{1}{c}\mathbf{V}_e \times \mathbf{B}\right) - m_e\nu_{ei}(\mathbf{V}_e - \mathbf{V}_i) - m_e\nu_{en}(\mathbf{V}_e - \mathbf{U}) = 0 \tag{3}$$

0094-8276/03/2003GL017418$05.00

$$\nabla \cdot \mathbf{J} = \nabla \cdot [n(\mathbf{V}_i - \mathbf{V}_e)] = 0 \tag{4}$$

where α denotes ion or electron species, n_α the density, m_α the mass, ν_{in} the neutral collision frequency, $\mathbf{U}$ is the thermospheric wind, ν_{ie}, ν_{ei} is the ion-electron and electron-ion Coulomb collision frequency, $\mathbf{E}$ the electric field with $\mathbf{E}_\perp = -\nabla_\perp \phi$ and $\mathbf{E}_\parallel = -\nabla_\parallel \phi$ with ϕ the electrostatic potential, $\mathbf{V}$ is the velocity, $\mathbf{g}$ is gravity, and ν_R is the recombination rate. The electron gyrofrequency is taken to be large compared to the electron collision frequency and electron inertial effects have been ignored. From equations (2), (3) the current $\mathbf{J}$ can be written $\mathbf{J} = \mathbf{J}_{ped} + \mathbf{J}_{hall} + \mathbf{J}_{pol} + \mathbf{J}_\parallel$ where

$$\mathbf{J}_{ped} = \sigma_p \left(\mathbf{E}_\perp + \frac{\mathbf{g} \times \mathbf{B}}{c\nu_{in}} + \frac{\mathbf{U} \times \mathbf{B}}{c} \right) \tag{5}$$

$$\mathbf{J}_{hall} = \sigma_H \left(-\frac{\mathbf{E}_\perp \times \mathbf{B}}{B} + \frac{B}{c\nu_{in}} \mathbf{g} + \frac{B_0}{c} \mathbf{U} \right) \tag{6}$$

$$\mathbf{J}_{pol} = c_m \left(\frac{\partial}{\partial t} + \mathbf{V}_i^0 \cdot \nabla \right) \left(\mathbf{E} + \frac{m_i}{e} \mathbf{g} \right) \tag{7}$$

$$\mathbf{J}_\parallel = \sigma_\parallel \mathbf{E}_\parallel \tag{8}$$

where $\sigma_p = (nec/B)(\alpha/(1+\alpha^2))$, $\sigma_H = \alpha\sigma_p$, $\sigma_\parallel = ne^2/m_e(\nu_{ei} + \nu_{en})$, $\alpha = \nu_{in}/\Omega_i$, $c_m = c^2/4\pi V_A^2$, and $\mathbf{V}_i^0 = (c/B^2)(\mathbf{E} + m_i\mathbf{g}/e) \times \mathbf{B}$. We include ion polarization $\mathbf{J}_{pol}$ currents to accurately treat the high altitude evolution of the bubble dynamics. Equation (8) adds parallel conductivity effects. Equation (1), (4) are solved using finite-difference numerical techniques. The MIDAS code has $200 \times 40 \times 30$ grid cells in the vertical, longitudinal, and parallel directions. The simulated region extends from an altitude of 120km in the northern hemisphere to an altitude of 120 km in the southern hemisphere with an apex height of 800 km. Equation (1) is solved using multi-dimensional flux corrected transport [*Zalesak*, 1979] while equation (4) is solved using an iterative solver. Since we consider only nighttime periods with the upper boundary to be less than 1000 km we keep only O^+, NO^+, and O_2^+. We have two versions of the model in both dipole and cartesian geometry. Here we present results using a dipolar geometry. The boundary conditions on the potential are Dirichlet at the bottom boundary and Neumann $\partial\phi/\partial y = 0$ at the top boundary in the vertical direction, periodic in the longitudinal direction, and set the potential to be zero at both ends of the flux tube. We use time-splitting method to treat the parallel and perpendicular dynamics. Since we consider bubble scale sizes greater than a few hundred meters (several hundred kilometers) in the perpendicular (parallel) directions, electron and ion pressure effects are not included since the time scales for parallel and perpendicular diffusive effects, for the scale sizes simulated in the model, are much longer than the time scales of interest. In the present study we set the thermospheric wind $\mathbf{U} = 0$. The two-dimensional version of the code has been applied to the evolution of ionospheric equatorial spread-F bubbles [*Keskinen et al.*, 1998].

[5] For the background ionosphere used to initialize the MIDAS code we use a modified SAMI2 model [*Huba et al.*, 2000]. SAMI2 treats the dynamical plasma and chemical evolution of several ion species, i.e., O^+, N_2^+, NO^+, O_2^+, H^+, He^+, N^+ in the altitude range of approximately 100 km to several thousand kilometers. SAMI2 includes ion inertial effects for accurate ion dynamics at high altitudes.

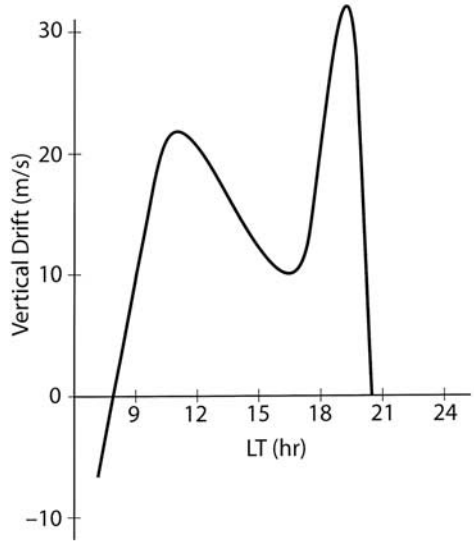

Figure 1. Vertical drift model used to generate initial background ionosphere.

3. Results

[6] In order to generate a background ionosphere with which to initialize the MIDAS model we use SAMI2 with a vertical drift model. We take a quiet time vertical drift model as shown in Figure 1. This is representative of equinoctial medium solar flux conditions [*Scherliess and Fejer*, 1999].

[7] Figure 2 gives the background F-region O^+ ionospheric conditions at 1900 LT at the longitude of Jicamarca Radio Observatory in Peru. As shown in Figure 2 equatorial anomaly crests are evident at approximately −24 and 9 degrees geographic latitude. The peak to trough ratio is approximately 1.8. Jicamarca is located at −12 degrees. The background E-region NO^+ ionospheric profile at the same local time was also computed using the SAMI2 model and used to initialize the MIDAS bubble simulation.

[8] We perturb the profile in Figure 2 with a 10 km sinusoidal density fluctuation with amplitude of 4 percent in the east-west direction. The form of the initial density perturbation along the magnetic field is found from computing the exact eigenfunction using linear theory with equation (1), (4) and the initial SAMI2 density profile. Figure 3 shows the nonlinear bubble evolution at t = 3850 sec. As can be seen the bubble has reached an altitude of approximately 750 km. Figure 4 shows the nonlinear evolution at the northern anomaly at t = 3350 sec. The F-peak is lower in altitude at the anomaly than at the equator, a manifestation of the equatorial plasma fountain. In addition the topside scale length is smaller than at the equator, i.e., the topside O^+ density falls off more quickly. We have found that the bubble structures grow slower at both the equator and anomaly when parallel conductivity effects are included. The growth times are slower than that predicted by local theory but faster than magnetic-flux-tube-integrated

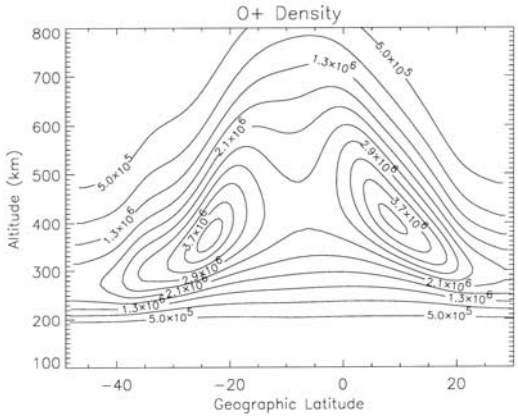

Figure 2. Plot of O^+ isodensity contours (in units of cm^{-3}) at t = 1900 LT from SAMI2 code.

model. The physical mechanism for the slower growth is that the parallel conductivity diverts part of the perpendicular ion Pedersen current, responsible for driving the Rayleigh-Taylor instability, into parallel electron current thus reducing the growth rate of the Rayleigh-Taylor instability. The generation of ionospheric structure at anomaly latitudes during equatorial spread-F as seen in these simulations is consistent with recent observational studies [*Basu et al.*, 2001a; *Basu et al.*, 2001b] showing indirectly, through radio scintillation effects, that strong ionospheric density gradients are occurring at equatorial anomaly latitudes in both quiet and stormtime periods during equatorial spread-F events. In addition recent optical studies of equatorial spread-F [*Otsuka et al.*, 2002] have demonstrated strong density depletions off the geomagnetic equator during equatorial spread-F events.

4. Summary

[9] We have presented the first study of the nonlinear three-dimensional evolution of an equatorial spread-F bubble. The initial background F-region and E-region ionosphere

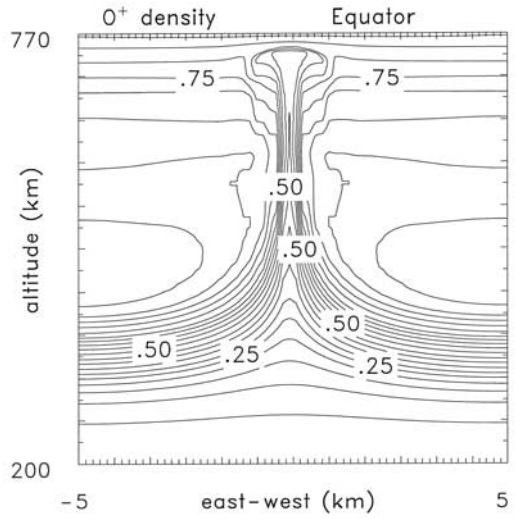

Figure 3. Plot of O^+ isodensity contours in nonlinear regime from MIDAS model. Densities have been normalized by $2.1 \times 10^6 cm^{-3}$. The time is t = 3350 sec.

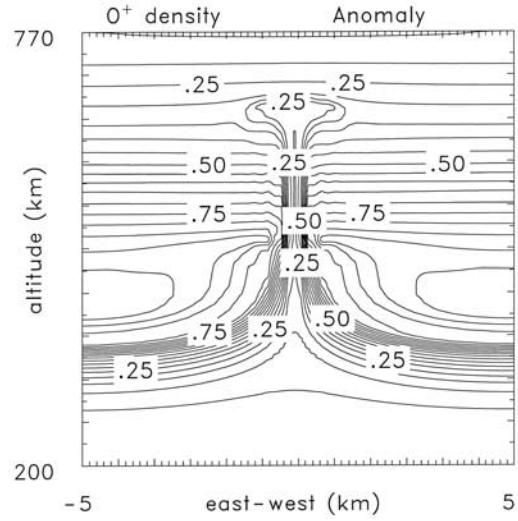

Figure 4. Plot of O^+ isodensity contours in nonlinear regime from MIDAS code. Densities have been normalized by $4.2 \times 10^6 cm^{-3}$. The time is t = 3108 sec. The latitude is 8 degrees.

is taken from a time-dependent equatorial plasma fountain model. We have found that finite parallel conductivity effects slow down the linear and nonlinear evolution of the equatorial spread-F bubble as compared with the two-dimensional evolution. In addtion, we find bubble-like structures can be generated at anomaly latitudes with extremely steep density gradients. Our results are consistent with recent radio and optical studies showing strong density gradients at anomaly latitudes during equatorial spread-F.

[10] In the future we hope to add the effects of thermospheric winds to the nonlinear evolution of three-dimensional spread-F bubbles and to study the higher altitude evolution of the spread-F bubbles.

[11] **Acknowledgments.** This work was supported by NASA. This work uses the SAMI2 ionosphere model written and developed by the Naval Research Laboratory.

References

Basu, Su., S. Basu, C. E. Valladares, H. C. Yeh, S. Y. Su, E. MacKenzie, P. J. Sultan, J. Aarons, F. J. Rich, P. Doherty, K. M. Groves, and T. W. Bullett, Ionospheric effects of major magnetic storms during the International Space Weather Period of September and October 1999; GPS observations, VHF/UHF scintillations, and in situ density structures at middle and equatorial latitudes, *J. Geophys. Res.*, *106*, 30,389, 2001a.

Basu, S., Su. Basu, K. M. Groves, H. C. Yeh, S. Y. Su, F. J. Rich, P. J. Sultan, and M. J. Keskinen, Response of the equatorial ionosphere in the South Atlantic region to the great magnetic storm of July, 15, 2000, *Geophys Res. Lett.*, *28*, 3577, 2001b.

Basu, S., E. Kudeki, Su. Basu, C. E. Valladares, E. J. Weber, H. P. Zengingonul, R. Sheehan, J. W. Meriwether, M. A. Biondi, H. Kuenzler, and J. Espinoza, Scintillations, plasma drifts, and neutral winds in the equatorial ionosphere after sunset, *J. Geophys. Res.*, *101*, 26,795, 1996.

Basu, B., On the linear theory of equatorial plasma instability: comparison of different descriptions, *J. Geophys. Res.*, *107*(A8), doi:10.1029/2001JA000317, 2002.

Chen, K. Y., H. C. Yeh, S. Y. Su, and C. H. Liu, Anatomy of plasma structures in an Equatorial spread-F event, *Geophys. Res. Lett.*, *28*, 3107, 2001.

Huang, C. S., M. C. Kelley, and D. L. Hysell, Nonlinear Rayleigh Taylor instabilities, atmospheric gravity waves, and equatorial spread-F, *J. Geophys. Res.*, *98*, 15,631, 1993.

Huang, C. Y., W. J. Burke, J. S. Machuzak, L. C. Gentile, and P. J. Sultan, DMSP observations of equatorial plasma bubbles in the topside ionosphere near solar maximum, *J. Geophys. Res.*, *106*, 8131, 2001.

Huba, J. D., G. Joyce, and J. A. Fedder, Sami2 is another model of the ionosphere (SAMI2): A new low-latitude ionosphere model, *J. Geophys. Res.*, *105*, 23,035, 2000.

Hysell, D. L., C. E. Seyler, and M. C. Kelley, Steepened structures in equatorial spread-F: Theory, *J. Geophys. Res.*, *99*, 8841, 1994.

Kelley, M. C., J. J. Makela, B. Ledvina, and P. M. Kintner, Observations of equatorial spread-F from Haleakala, Hawaii, *J. Geophys. Res.*, *29*(20), doi:10.1029/2002GL015509, 2002.

Keskinen, M. J., S. L. Ossakow, S. Basu, and P. Sultan, Magnetic flux tube integrated evolution of equatorial ionospheric plasma bubbles, *J. Geophys. Res.*, *103*, 3957, 1998.

Keskinen, M. J., S. L. Ossakow, and P. K. Chaturvedi, Preliminary report of numerical simulations of intermediate wavelength collisional Rayleigh Taylor instability in equatorial spread-F, *J. Geophys. Res.*, *85*, 1775, 1980.

Kil, H., and R. A. Heelis, Global distribution of density irregularities in the equatorial ionosphere, *J. Geophys. Res.*, *103*, 407, 1998.

Otsuka, Y., K. Shiokawa, T. Ogawa, and P. Wilkinson, Geomagnetic conjugate observations of equatorial airglow depletions, *Geophys. Res. Lett*, *29*(15), doi:10.1029/2002GL015347, 2002.

Sahai, Y., P. R. Fagundes, and J. A. Bittencourt, Transequatorial F-region ionospheric plasma bubbles: Solar cycle effects, *J. Atmos. Terr. Phys.*, *62*, 1377, 2000.

Scannapieco, A. J., and S. L. Ossakow, Nonlinear spread-F, *Geophys. Res. Lett.*, *3*, 451, 1976.

Sinha, H. S., S. Raizada, and R. N. Misra, First simultaneous in situ measurement of electron density and electric field fluctuations during spread-F in the Indian zone, *Geophys. Res. Lett.*, *26*, 1669, 1999.

Scherliess, L., and B. G. Fejer, Radar and satellite global equatorial F region vertical drift model, *J. Geophys. Res.*, *104*, 6829, 1999.

Sekar, R., R. Suhasini, and R. Ragvaharo, Evolution of plasma bubbles in the equatorial F-region with different seeding conditions, *Geophys. Res. Lett.*, *22*, 885, 1995.

Stephan, A. W., M. Colerico, M. Mendillo, B. W. Reinisch, and D. Anderson, Suppression of equatorial spread-F by sporadic E, *J. Geophys. Res.*, *107*(A2), doi:10.1029/2001JA000162, 2002.

Weber, E. J., et al., Equatorial plasma depletion precursor signatures and onset observed south of the magnetic equator, *J. Geophys. Res.*, *101*, 26,829, 1996.

Yeh, H. C., S. Y. Su, and R. A. Heelis, Storm time plasma irregularities in the pre-dawn hours observed by the low latitude ROCSAT-1 satellite at 600 km altitude, *J. Geophys. Res.*, *28*, 685, 2001.

Zalesak, S. T., S. L. Ossakow, and P. K. Chaturvedi, Nonlinear equatorial spread-F: The effect of neutral winds and background Pedersen conductivity, *J. Geophys. Res.*, *87*, 151, 1982.

Zalesak, S. T., Fully multidimensional flux corrected transport algorithms for fluids, *J. Comput. Phys.*, *31*, 355, 1979.

M. J. Keskinen, Charged Particle Physics Branch, Plasma Physics Division, USA.

S. L. Ossakow, Plasma Physics Division, Naval Research Laboratory, Washington, DC 20375, USA.

B. G. Fejer, Center for Atmospheric and Space Studies, Utah State University, Logan, UT, USA.